# SUPPLEMENTAL MATERIAL

## The predicted RNA-binding protein regulome of axonal mRNAs

Raphaëlle Luisier[1,2*], Catia Andreassi[3*], Lisa Fournier[1,2] and Antonella Riccio[3]

[1]Idiap Research Institute, Martigny 1920, Switzerland.

[2]SIB Swiss Institute of Bioinformatics, Lausanne 1015, Switzerland.

[3]UCL Laboratory for Molecular Cell Biology, University College London, London WC1E 6BT, UK.

Corresponding authors: a.riccio@ucl.ac.uk, raphaelle.luisier@idiap.ch

*These authors contributed equally to the work

### 1. Supplemental Results

**Localisation score and abundance ratios comparisons**

While the 3' end sequencing itself is independent of the length of the transcript, our data demonstrate that the efficiency in transport is not. Indeed we find that smaller transcripts have higher chances of localising in the axons (**Supplemental Fig. S4D**). Furthermore we also find that above a certain level of expression in the cell body, the probability to be detected in distal axons is 1.0 (**Supplemental Fig. S4C**).

Classic approaches utilise the abundance ratios between axons and cell bodies to quantify 3' UTR isoform axonal transport and identify excess in these values associated with over-localisation, similarly to the localisation score. As shown in **Supplementary Fig. S4F,G** (*upper*) there is a dependency between the ratios of the reads between axons and cell body and expression in the cell body or transcript length (upper panels). Thus with this metric, highly expressed transcripts have higher chances to be detected as differentially localized compared to those expressed at a lower level, given the larger dynamic ranges of the former. Similarly smaller transcripts have a better chance to be detected as transported compared to larger transcripts. This is shown in the **Supplemental Fig. S4H**: in (*upper pane*l) the differentially localized 3' UTR isoforms between NGF and NT-3 are identified using the difference in abundance rations while in (*lower panel*) they are identified based on difference in localization scores. In (*upper panel*) we observed a depletion of differentially localized isoforms in the lowly expressed 3' UTR isoforms in the cell body, which is not the case in (*lower panel*).

The localization score was developed to identify 3' UTR isoforms either restricted to the cell body or transported in excess to the axonal compartment, while accounting for transcript length and basal transcriptional level, two parameters that we showed to directly relate to the likelihood of being detected in axonal compartment (**Supplemental Fig. S4C,D**). As shown in **Supplemental Fig. S4F,G** (*upper panels*), the median abundance ratios between axons and cell body directly depends on both of these parameters, and indeed the red line is not centered on zero but fluctuates according to these values. This is in contrast with the localisation score where the median localisation score is centered on zero along the dynamic ranges of expression in cell body and transcript length (*lower panels*). Thus these dependencies are corrected with the new scoring approach (lower panels) where the red lines (indicating median abundance ratios between cell body and axons, and median localisation, respectively) are centered on zero. Overall the localisation score performs better in identifying lowly expressed transcripts exhibiting changes in localisation compared to abundance ratios.

A second limitation of this metric, that is addressed with the newly developed localisation score, is that the dynamic ranges for the ratios in abundance are directly related to the abundances in the cell body i.e. highly expressed transcripts have larger dynamic ranges in abundance rations and are more likely to be associated with extreme values which do not necessarily mean active transport or cell body restriction. Indeed comparing the GO enrichments for *defined ranges of abundance ratios* in NGF samples *(***Supplemental Fig. S7A***)* versus *defined ranges of localisation scores (***Supplemental Fig. S7B***)* shows that terms associated with over-transported transcripts using LS scores better reflect the biological system (axon development, cell adhesion). In contrast, in **Supplemental Fig. S7A** identified terms are associated with translation, due the high level of expression of the related genes in this system.

In conclusion LS enables the identification of over- and under-transported mRNA irrespective of the expression levels and provides a better statistical tool than the ratio of the gene abundance between axons and cell bodies commonly used to quantify mRNA localisation.

## 2. Supplemental Methods

### RNA isolation, reverse transcription, linear amplification and 3'end-RNA-seq

To ensure that the axons were free of cell bodies, prior to each experiment axon compartments were incubated with Hoechst 33342 (10µg/mL in PBS for 20 min at 37˚C) and observed under an inverted fluorescent microscope. Cultures showing cell nuclei in the axon compartments or leakage of the dye in the central compartment were discarded. Total axonal and cell bodies RNA was purified from the lateral compartments of 52 or 36 chambers for

the NGF samples, or of 12.5 chambers each for the NT-3 samples, and from the central compartment of 7 or 6 chambers for each cell body sample, obtained from 3 or more independent cultures. Total RNA was isolated using PureLink® RNA Micro Scale Kit, according to the manufacturer's instructions with minor modifications. Briefly, axons and cell bodies were collected from chambers using a lysis buffer (300µL) containing 10%β-mercaptoethanol. Total mRNA bound to the columns was washed and eluted twice in elution buffer (12µL). Aliquots of each sample were reverse transcribed in a 20µL reaction volume containing random hexamer mix and 50U SuperScript III Reverse Transcriptase at 50°C for 1 hr. To check the quality of samples and the absence of cell bodies contamination in axon samples, first-strand cDNAs (5µL) were PCR amplified in a 25µL PCR reaction containing actin beta or histone H4 specific primers (0.20µM), dNTPs (200 nM) and Go Taq polymerase (1.25U, Promega). Primer sequences and PCR conditions are provided (**Table S23**).

For mRNA linear amplification, samples were purified as described above, concentrated by speed-vacuum centrifugation to 1µL (axons) or 5µL (cell bodies) volume, and used for two rounds of linear amplification as previously described (Baugh et al. 2001). For the first round of amplification, a custom-made degenerated oligo-d(T) primer (MWG) carrying a T7 promoter sequence was used. The volume of the first-strand reaction for the axons was scaled down to 5µL. After the second round of amplification carried out with random hexamers (ThermoFisher Scientific), contaminant cDNA was digested by treating the samples with RNAse-free DNase (2U, Epicentre). Performance of the samples was tested by RT-PCR. Linear amplified aRNA from cell bodies and axon samples (2 biological replicates each) was used to prepare RNA-seq libraries using the strand-specific ScriptSeq protocol. Paired-end sequencing (2x 150bp) of four indexed libraries was performed on the Illumina HiSeq 2000 platform, generating in excess of 80M mappable reads per sample. Library preparation and sequencing were performed at the Liverpool Centre for Genomic Research (CGR, http://www.liv.ac.uk/genomic-research/). Primer sequences are described in **Table S23**. All raw and processed sequencing data used in this study have been previously submitted to the NCBI Gene Expression Omnibus (GEO; https://www.ncbi.nlm.nih.gov/geo/) under accession number GSE160025 (Andreassi et al. 2021).

**RT-PCR and quantitative RT-PCR**

For validation of the 3'end seq, mRNA was isolated as described above from independent cultures of sympathetic neurons and reverse transcribed. qRT-PCR reactions (25µL) contained 12.5µL of Sybr Select or Luna (NEB) Mastermix and 0.25 µM primers, unless otherwise indicated. Reactions were performed in triplicate on a Biorad CFX Connect Real-time Machine. The Comparative Ct Method (ΔΔCt Method) was used for relative

quantification. At the end of 40 cycles of amplification, a dissociation curve was performed in which SYBR Green fluorescence was measured at 1ºC intervals between the annealing temperature and 100ºC. Peaks of the melting temperatures of amplicons varied between 80ºC and 90ºC. Primer sequences and PCR conditions are described in **Table S23**.

**Single molecule FISH (smFISH)**

Probe sets targeting the 3'UTR of rat *Atf3* (Stellaris probes, Biosearch technologies) were designed using the Stellaris probe-set designer tool to specifically detect the 3'UTR of the transcript and 3'end labelled with CalFluor590. Probes were reconstituted at 12.5μM in TE buffer (10mM Tris pH8, 1mM EDTA pH8). smFISH was performed as previously described (Andreassi et al. 2021) on SCG neurons cultured on glass coverslips for 5 days in high NGF concentration (100ng/mL) and then either maintained in high NGF or washed and maintained in NT-3 (1μg/mL) for further 7 days before fixation. Cells were washed with PBS, fixed using 3.7% PFA at RT for 10 mins, permeabilised with 70% EtOH at 4°C for 3.5 hrs and then pre-hybridised in 2xSSC 10% Formamide for 5mins at RT. 1μl of 12.5μl probe stock was added to 100μl Hybridisation buffer (10% Dextran Sulfate, 2xSSC, 10% Formamide, 2mM vanadyl ribonucleoside, 0.1ug/uL salmon sperm DNA, 0.1% Triton X-100, 1% BSA) before incubation of the coverslips O/N at 42°C in humidified chamber. Coverslips were then washed 2x30 mins in warm 2xSSC 10%Formamide at 37°C in the dark and 1x5 min in PBS+100ug/mL DAPI before mounting to slides with ProlongGold. Coverslips were cured O/N at RT before imaging at a 3i confocal microscope (Intelligent Imaging Innovations, Inc.) equipped with a Photometrics Prime 95B (Scientific CMOS) camera. Images were processed using ImageJ software. Maximum intensity projection of the image stacks were generated before adjusting brightness and contrast. The image was then converted to 8- bit and pseudo-coloured using the Fire look-up table to facilitate visualisation of the signal level, before changing the image type to RGB colour. Figures of the tiff files were prepared using Adobe Photoshop and Adobe Illustrator software.

**Inference of 3'UTR isoforms from 3'-end RNA-seq**

The rat genome is poorly annotated compared with mouse and human; therefore, 3′ end RNA-seq data were used to identify unknown isoforms by re-annotating the 3′ ends to the Ensembl Rn5 database (v.78) as previously described (Andreassi et al. 2021). Briefly paired-end stranded RNA-seq reads of 150 bp were mapped to the reference rat genome (UCSC, rn5), and nucleotide-level stranded coverage obtained for axons and cell body enabled the identification of continuously transcribed regions. Continuously expressed fragments were next associated with matching strand overlapping 3'UTR using Ensembl

version 78 (v78) (Flicek et al. 2013), and extensive downstream filtering was performed to exclude potential intragenic transcription, overlapping transcripts, and retained introns as described in (Miura et al. 2013). Segmentor3IsBack R package was finally used to segment the longest 3' UTR isoform in regions of spatially coherent coverage hence to identify alternative 3'UTR isoforms (Cleynen et al. 2014). 3' ends located within 50 nt distance were clustered together, selecting the most promoter-distal annotation. The GTF annotation file was deposited together with the source code to generate the new 3' UTR annotation on GitHub : https://github.com/RLuisier/my3UTRs. The version Rn5 of the rat genome was used as this study is an extension of our previous one (Andreassi et al. 2021). At the release of the Rn6 Ensembl annotation, we carefully compared our 3' UTR novel annotation with Rn6 and found that 19% of our novel 3' UTR isoforms were in a [-100;100] nt window of the closest 3' UTR in Rn6. We also compared the extent of lengthening between our new annotation and Rn5 *versus* Rn6 and found that Rn6 does not significantly extend 3' UTR length. Additionally, while 26% of the newly annotated 3' UTR isoforms were at the exact same distance of the nearest 3' UTR in either Rn5 and Rn6 and 52% within 10 nt distance from each other, the distance to the nearest 3' UTR in either annotation is almost equivalent. In view of the relative high similarity of the 3' UTR isoforms between Rn5 and Rn6, the use of Rn6 is not expected to change the key results in our manuscript, in particular the findings that 1) 3' UTR isoforms targets to the axonal compartment are longer than those restricted to the cell body, and 2) at least 100 short 3' UTR isoforms are uniquely detected in the distal axons.

**Analysis of Alternative cleavage and polyadenylation (APA)**

In order to systematically investigate the changes in the poly(A) site usage between conditions we first scored the log2 proximal-to-distal poly(A) site ratio in each compartment or condition and each individual biological replicate by taking the log2 ratio of promoter-proximal and promoter-distal 3' UTR isoform expression levels, hereafter called RUD. A score higher than 0 therefore indicates higher abundance of promoter-proximal 3'UTR isoform in the compartment or condition of interest. In the case of multiple promoter-distal 3' UTR isoforms per transcript ID, a value was computed for each individual promoter-distal 3' UTR isoform i.e. several values could be obtained per transcript ID family. We also computed the relative 3' UTR usage between the promoter-proximal and the promoter-distal 3' UTR isoform by calculating the ratios between the read count in the promoter-proximal and the sum of the read counts in the promoter-proximal and the promoter-distal 3' UTR isoforms, hereafter called PUD.

In order to identify tandem 3' UTR that show a marked change in the use of promoter proximal and distal poly(A) sites either between NGF and NT-3 in the cell body or between cell body and axons in either NGF or NT-3, we restricted our analysis on transcript ID

families containing at least two 3' UTR isoforms, and for which at least one promoter-distal 3' UTR isoform was expressed in at least one of the compared conditions. In order to identify transcripts that show a marked change in the pA site usage between conditions, we scored the differences in proximal-to-distal poly(A) site usage using the following two scores:

$$\Delta_{RUD} = log2\left(\frac{I_{proximal}}{I_{distal}}\right)_{cond1} - log2\left(\frac{I_{proximal}}{I_{distal}}\right)_{cond2} = RUD_{cond1} - RUD_{cond2}$$

$$\Delta_{PUD} = \frac{I_{proximal}}{I_{proximal}+I_{distal}}_{cond1} - \frac{I_{proximal}}{I_{proximal}+I_{distal}}_{cond2} = PUD_{cond1} - PUD_{cond2} \in [-1, 1]$$

The statistical significance of the changes in proximal-to-distal poly(A) site ratio between conditions was assessed by Fisher's exact count test using summed-up raw read counts of promoter-proximal *versus* promoter-distal 3' UTR isoforms originating from either conditions (cell body versus axonal compartment or cell bodies of NGF *versus* NT-3 conditions). We adjusted the P-Value controlling for False Discovery Rate (FDR) of 0.01. We restricted our analysis on Ensembl transcripts containing at least two 3' UTRs generated by tandem polyadenylation expressed in either condition. Proximal shifts were then selected when $\Delta_{RUD} \leq -1$, $\Delta_{PUD} \leq -15\%$ and FDR<0.01; distal shifts were selected when $\Delta_{RUD} \geq 1$, $\Delta_{PUD} \geq 15\%$ and FDR<0.01.

**Differential gene expression analysis**

For this analysis we focussed on the data obtained from the cell body compartments. The pipeline described above outputs 3' UTR transcript abundance, and thus we first calculated the abundance of genes by summing up the estimated raw count of the constituent isoforms to obtain a single value per gene. Differential analysis was performed using the edgeR package (Robinson et al. 2010). Normalization factors were computed using the TMM technique, after which tagwise dispersions were calculated and subjected to an exact test. Resulting P values were subjected to Benjamini–Hochberg multiple testing correction to derive FDRs. Genes were considered as differentially expressed between NGF and NT-3 if log2FC>0.58 (FC>1.5) and P value <0.01. The complete lists of differentially expressed genes are reported in **Supplemental Tables S1,S2**.

**Transcription Factor Binding Site analysis**

The 1000 nucleotide promoter region surrounding the transcription start site of the human genome (GRCh38) of each gene was screened for transcription factor binding site (TFBS) regulatory motifs using the Bayesian regulatory site prediction algorithm MotEvo (Arnold et al. 2012), which incorporates information from orthologous sequences in six other mammals and uses explicit models for the evolution of regulatory sites. The 190 regulatory motifs represent binding specificities of roughly 350 different human TFs. These were lifted to rn5

using liftOver (Hinrichs et al. 2006). The predicted number of functional TFBSs for each promoter was summed and used to perform Fisher Enrichment analysis between the genes up-regulated in NGF and NT-3 conditions. The result of this analysis is presented in **Supplemental Table S3**.

## 3. Supplemental Figures

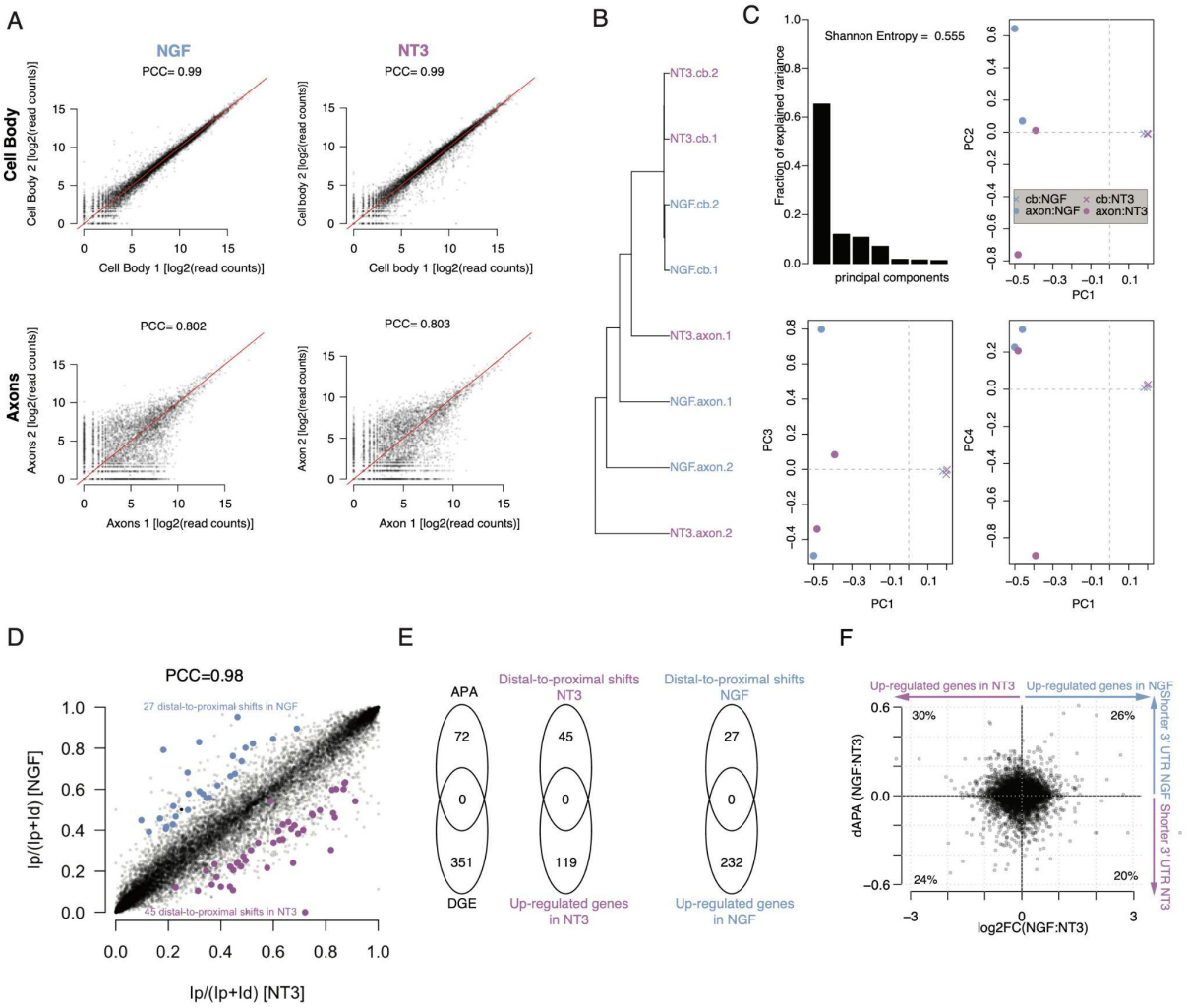


**Supplemental Figure S1.** *(A)* Scatterplot of the gene expression level between technical replicates. PCC=pearson correlation score. *(B)* Unsupervised hierarchical clustering of 12,285 3' UTR isoforms in n = 8 samples (cell body and axons in two culture conditions). Distance is 1 minus Spearman rank correlation. Complete clustering. *(C)* Singular value decomposition analysis of 12,285 3' UTR isoforms in n = 8 samples. (*upper left*) Barplot of the fraction of variance captured by the 8 principal components. Scatter plots of the samples in the first four principal components (*upper right:* PC1 and PC2; *lower left:* PC1 and PC3; *lower right*: PC1 and PC4). Blue and purple points indicate projection of the NGF samples and for the NT-3 samples respectively. Cross and circles indicate projection of the cell body and axonal samples respectively. *(D)* Scatterplot of the relative usage of promoter-proximal and promoter-distal 3' UTR isoform in cell bodies of neurons exposed to either NGF or NT-3 (FDR < 0.01 between NGF and NT-3; Fisher's exact test). Proximal shifts in NGF compared to NT-3 (blue); proximal shifts in NT-3 compared to NGF (purple). *(E)* Venn diagrams comparing the lists of differentially expressed genes and genes exhibiting alternative

polyadenylation between NGF and NT-3 culture conditions. *(F)* Scatter plot comparing the changes in gene expression and the changes in 3' UTR between NGF and NT-3. Percentage in each quadrant indicates the number of genes in each quadrant divided by the number of total examined genes.

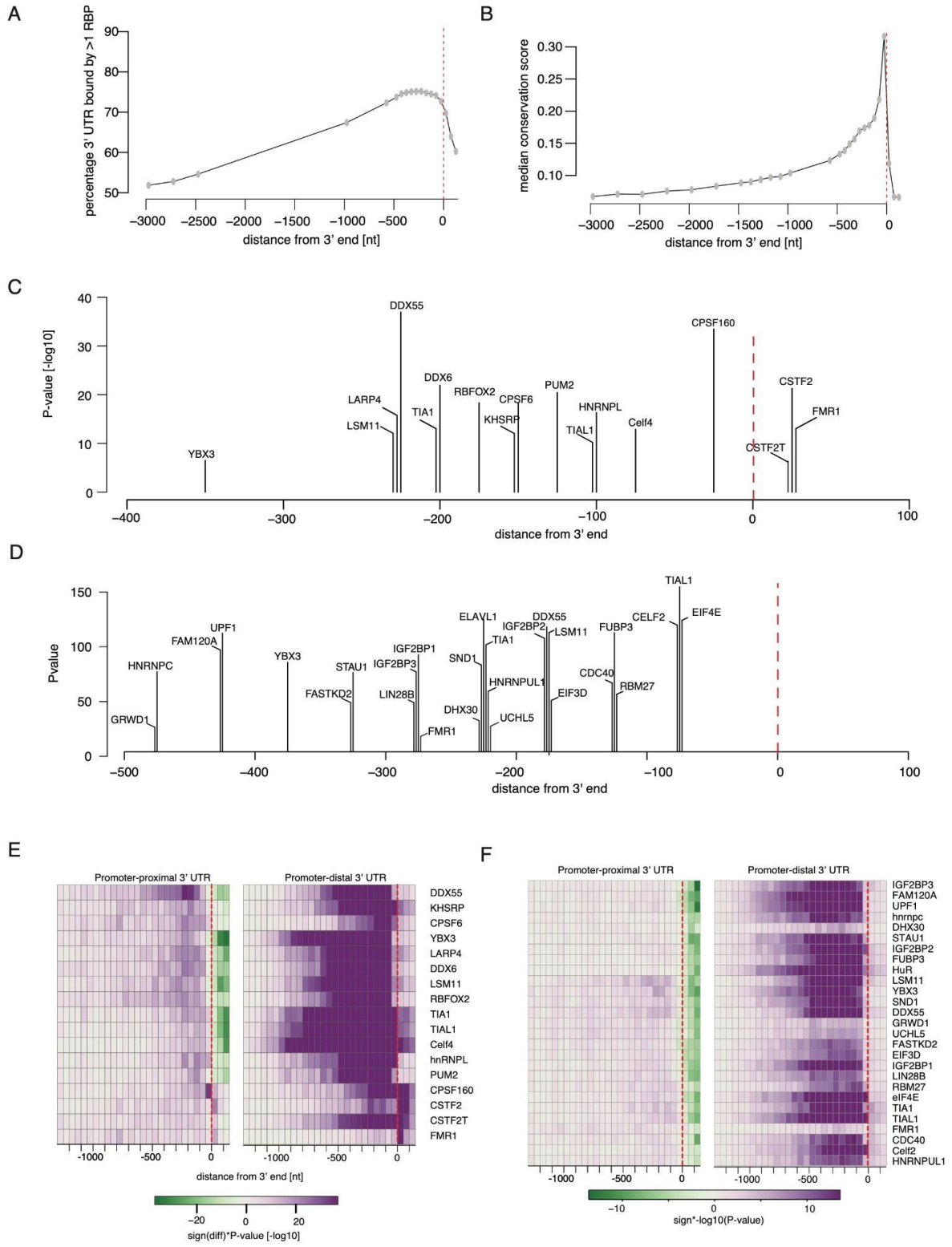


**Supplemental Figure S2.** *(A)* Analysis of the percentage of 3' UTR isoforms exhibiting cross-link event for at least one RBP as a function of the distance to the 3' end. *(B)* Analysis of the nucleotide conservation score of 3' UTR isoform in function of the distance to the 3'

end. *(C)* Position-dependent significance in positive association between cross-link events in defined regions along the short and long 3’ UTR for 17 identified positive regulators of polyadenylation. *(D)* Position-dependent significance in positive association between cross-link events in specific regions along the promoter-distal 3’ UTR for 27 identified positive regulators of long 3’ UTR and negative regulators of short 3’ UTR isoform. *(E)* Heatmap showing the extent of region-specific association between cross-link events for the individual 17 candidate positive regulators of polyadenylation and the relative usage of the proximal (*left*) or distal (*right*) 3’ UTR isoform. *(F)* Heatmap showing the extent of region-specific association between cross-link events for the individual 27 candidate negative regulators of promoter-proximal 3’ UTR isoforms and the relative usage of the proximal (*left*) or distal (*right*) 3’ UTR isoform.

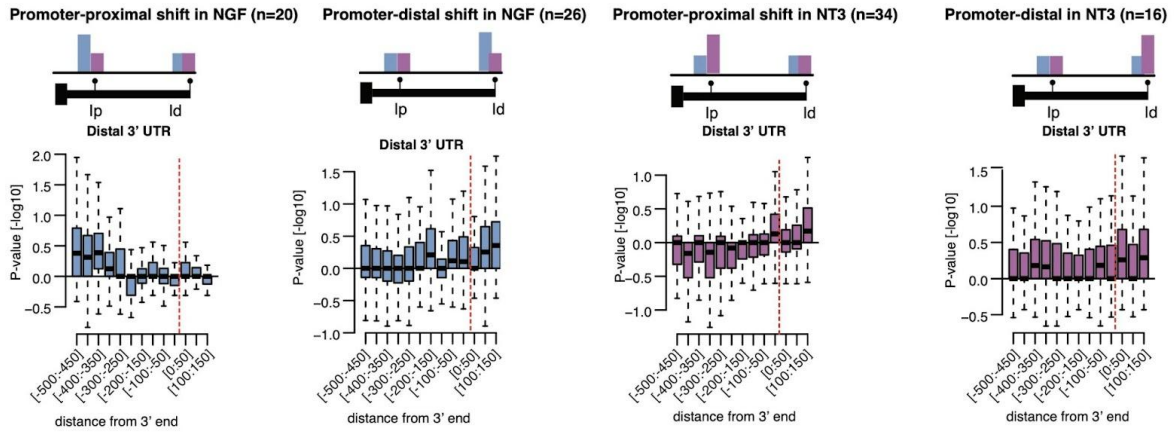


**Supplemental Figure S3.** Distribution of Fisher enrichment scores ($-\log_{10}$(P-value)) in RBP cross-link events along the long 3' UTR isoforms of the pairs of isoforms exhibiting significant promoter-proximal shift or promoter-distal shift in NGF, and promoter-proximal shift or promoter-distal shift in NT-3.

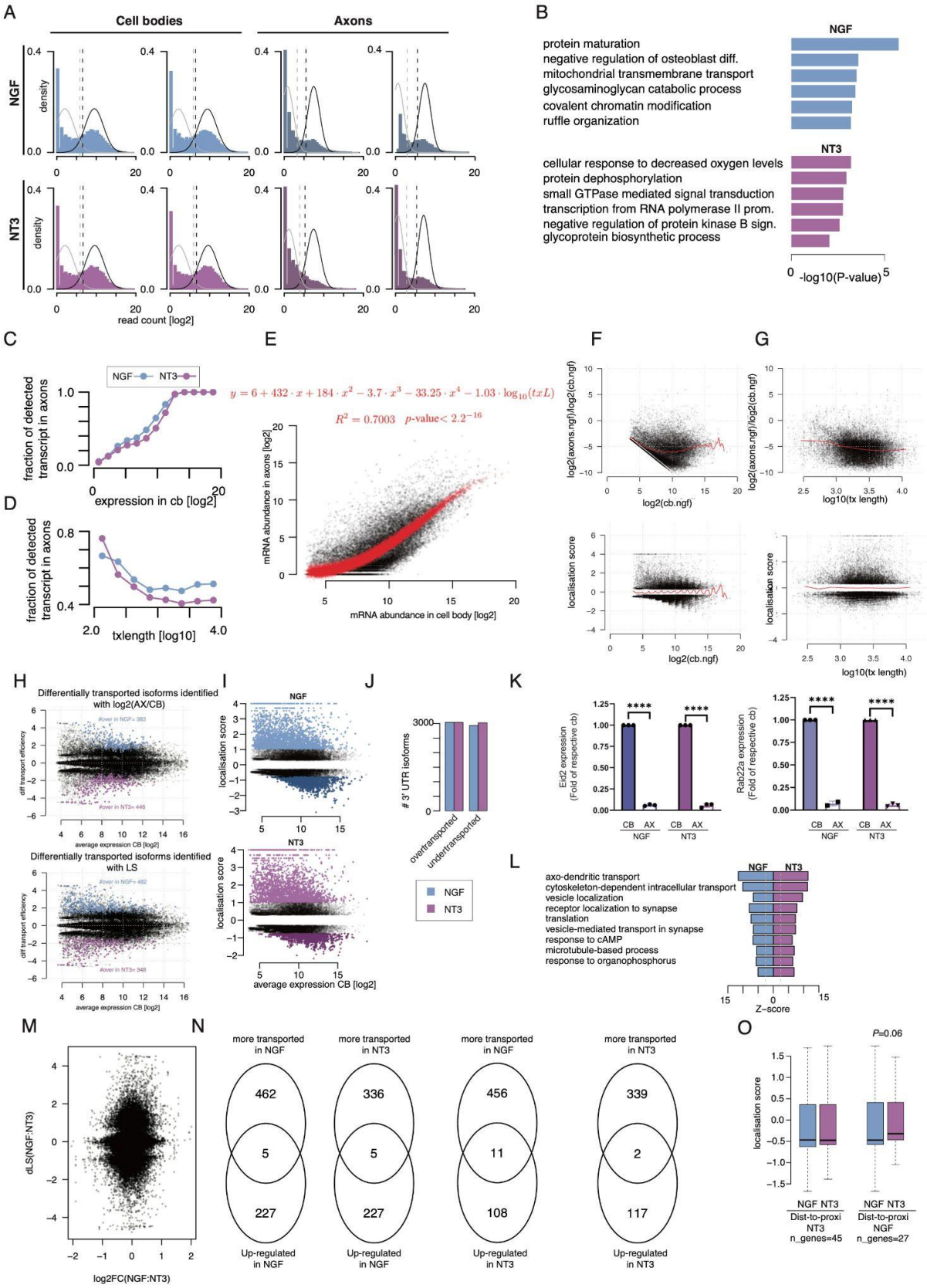


**Supplemental Figure S4.** *(A)* Bimodal distribution of the $\log_2$-read count in cell bodies and distal axonal samples. Dotted lines indicate the upper (stringent) and lower (loose) limits to discriminate the background gene expression level from the foreground. *(B)* GO biological

pathway enrichment for genes detected in the distal axons of NGF (blue) or NT-3 (purple) culture conditions only. *(C)* Fraction of transcripts detected (i.e reliably expressed) in the axonal compartment in function of the mRNA abundance in the cell body ($log_2$) showing that the probability for a 3' UTR isoform to be detected in the axonal compartment depends on its level of expression in the cell body compartment. To generate this figure all transcripts exhibiting a reliable level of expression in the cell body compartment were considered, and for each range of cell body expression (read count), we have counted which fraction exhibit a reliable level of expression in the axonal compartment. *(D)* Fraction of detected transcripts in the axonal compartment in function of the transcript length ($log_{10}$) showing that the probability for a 3' UTR isoform to be detected in the axonal compartment depends on its length in nucleotides. *(E)* Relationship between the mRNA abundance in cell bodies ($log_2$) and in distal axons ($log_2$). A linear model is fitted that predicts the axonal mRNA abundance in function of the transcript length ($log_{10}$) and of a polynomial of degree 4 of the abundance in the cell bodies (red equation). *(F)* Average mRNA abundance in the cell bodies ($log_2$) and the ratios between the axonal and cell body mRNA abundance ($log_2$; *upper*) or as compared with the localisation scores (*lower*). Red lines = average ratios (*upper*) or localisation scores (*lower*) per range of cell body abundance. *(G)* Transcript length ($log_{10}$) and the ratios between the axonal and cell body mRNA abundance ($log_2$; *upper*) or as compared with the localisation scores (*lower*). Red lines = average ratios (*upper*) or localisation scores (*lower*) per range of cell body abundance. *(H)* Comparison of the dependence on expression level in the cell body of the detected differentially localised transcripts between NGF and NT-3 either using the ratios in abundance between cell body and axons (*upper*) versus the localisation score (*lower*). *(I)* Localisation score and average mRNA abundance in the cell bodies of NGF- (*upper*) or NT--treated neurons (*lower*). Dark dots=under-transported and light dots=over-transported. *(J)* Number of 3' UTR isoforms exhibiting excessive axonal localisation (over-transported) as well as restricted to the cell bodies (under-transported) in either NGF or NT-3 culture conditions. *(K) (left) Eid2* and (right) *Rab22a* mRNA abundance in cell bodies and axons as measured by RT-qPCR (unpaired *t*-test, n=2 or 3 as indicated, ****p<0.0001). *(L)* Standardized scores (*Z*-score) quantifying the excess in axonal localisation in NGF and NT-3 for the top ten GO biological pathways. *(M)* Scatter plot comparing the changes in the gene expression and the differences in axonal localisation scores between NGF and NT-3 conditions. *(N)* Venn diagram comparing the differentially expressed genes and the differentially transported transcripts between the two conditions. *(O)* Localisation scores of the transcripts whose genes exhibit significant 3' UTR shortening in NT-3 *versus* NGF (left) and NGF *versus* NT-3 (right). P-value=Welch's *t*-test.

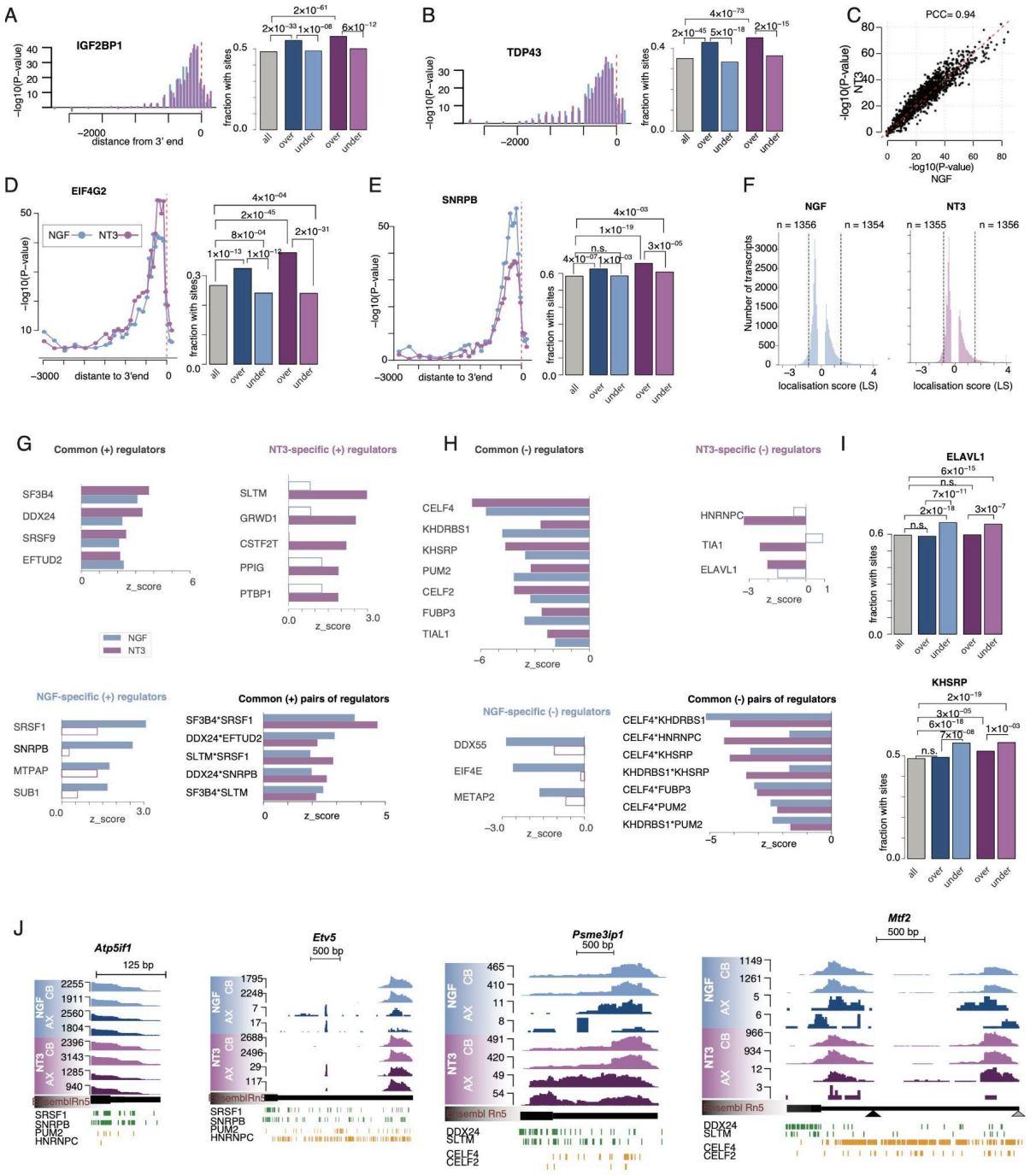


**Supplemental Figure S5.** *(A, left)* Significant association between IGF2BP1 cross-link event and axonal localisation in defined regions along the 3' UTR . Blue = NGF; purple = NT-3. (*Right*) Barplots showing the fraction of [-250:-50] nucleotide regions upstream the 3' ends exhibiting IGF2BP1 cross-link event in the full set of detected transcript (grey bar), and the pools of over- and under-transported transcripts in NGF (blue bars) and NT-3 (purple bars), respectively. P-value from Fisher enrichment test. *(B)* Same as *(A)* for TDP43. *(C)* Comparison of the significance in association between the 126 RBPs cross-link events in the [-250:-50] nt region upstream the 3' end and the axonal localisation in NGF *versus* NT-3. *(D, E)* Same as (A) for EIF4G2 and SNRBP. *(F)* Selection of the 5% transcripts exhibiting

highest and lowest axonal localisation scores in NGF (*left*) and NT-3 (*right*) culture conditions respectively used for the development of the machine learning classifiers. (*G*) Barplot showing the significant positive RBPs that significantly contribute to M1 classifier in NGF and NT-3 conditions (*upper left*), in NGF condition only (*lower left*), in NT-3 condition only (*upper right*), and positive pairs of RBPs in both NGF and NT-3 conditions (*lower right*). (*H*) Same as (*G*) for significant negative RBPs. *(I)* Barplots showing the fraction of [-250:-50] nucleotide regions upstream the 3' ends exhibiting ELVAL1 (*upper*) and KHSRP (*lower*) cross-link event in the full set of detected transcript (grey bar), and the pools of over- and under-transported transcripts in NGF (blue bars) and NT-3 (purple bars), respectively. P-value from Fisher enrichment test. *(J)* Genome browser views of 3' end sequencing profiles and CLIP crosslinking events for predicted positive (green) and negative (gold) regulators of axonal localisation for 3' UTR isoforms exhibiting excess in axonal localisation or restriction to the cell body.

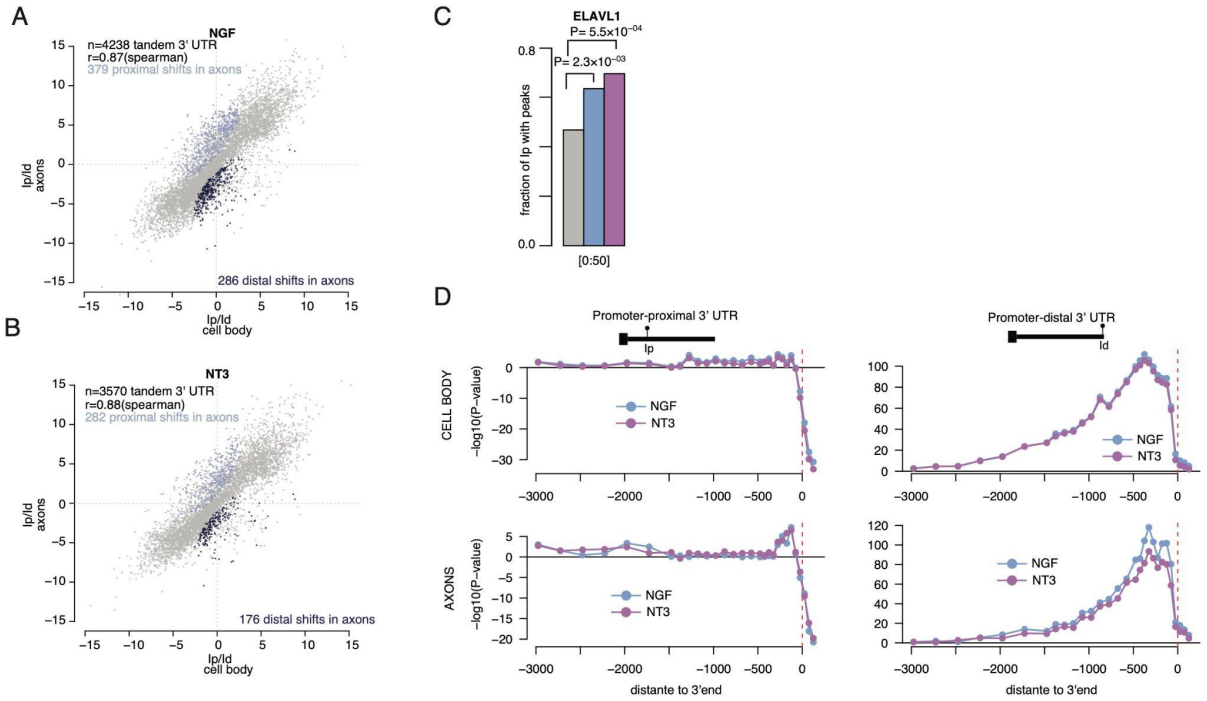


**Supplemental Figure S6.** *(A)* Scatterplot of the relative usage of promoter-proximal and promoter-distal 3' UTR isoforms sites in cell bodies and axons of NGF-treated condition (FDR < 0.01 between cell body and axonal compartment; Fisher's exact test). Distal shifts in axons compared with cell body (dark blue); proximal shifts in axons compared with cell body (light blue). *(B)* Same as *(A)* for NT-3 treated condition. *(C)* Fraction of promoter-proximal 3' UTR isoforms exhibiting cross-link events for ELAVL1 in [0:50] nucleotide region down-stream of the cleavage site. Gray bar = all promoter-proximal 3' UTR; blue bars = 80 candidates of axonal remodeling in NGF; purple bars = 60 candidates of axonal remodeling in NT-3. *(D)* Scatterplot of the extent of significant association between UPF1 cross-link event in defined regions along the 3' UTR and the relative usage of the promoter-proximal 3' UTR (*left*) or the promoter-distal 3' UTR (*right*) in the cell body (*upper*) or the axons (*lower*). Blue = NGF; purple = NT-3.

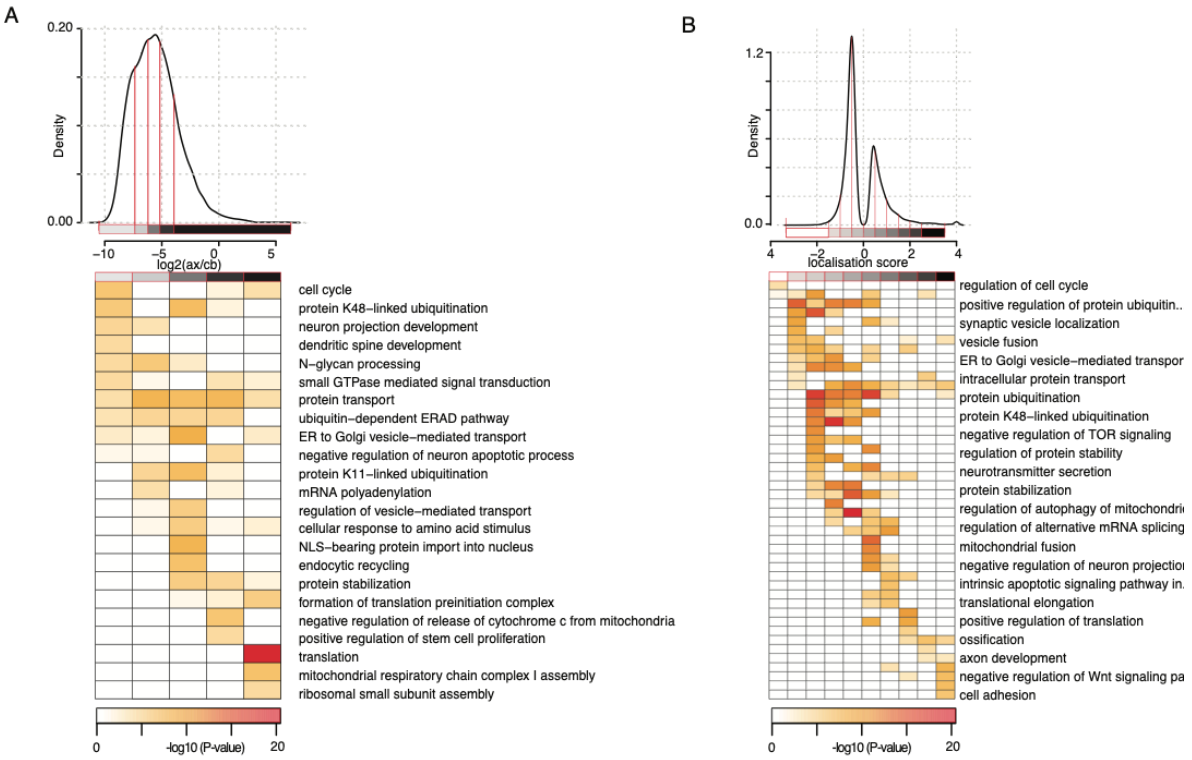


**Supplemental Figure S7.** (*A*). (*upper*) Distribution of the 3' UTR isoforms ratios in average abundance between the axonal compartments and the cell bodies. 3' UTR isoforms were clustered in 5 different ranges of abundance ratios of similar size. (*lower*) Heatmap of the GO biological pathway enrichment for the five groups of 3' UTR isoforms of specific range of abundance ratios between axons and cell bodies. Fisher enrichment test. (*B*). Same as (A) with 3' UTR isoforms grouped according to localisation score.

## 4. Supplemental Tables

Table S1 : **Up-regulated genes in NGF treated cells compared to NT-3.** Columns represent: 1-Ensembl Rn5 transcript ID, 2- gene symbol, 3- difference in gene expression level between NT-3 and NGF (log2FC), 4- average gene count per millions across all samples (log), 5- adjusted (FDR) P-value.
https://zenodo.org/record/8189110/files/Supplemental%20Table%20S1.xlsx?download=1

Table S2 : **Up-regulated genes in NT-3 treated cells compared to NGF.** Columns represent: 1-Ensembl Rn5 transcript ID, 2- gene symbol, 3- difference in gene expression level between NT-3 and NGF (log2FC), 4- average gene count per millions across all samples (log), 5- adjusted (FDR) P-value.

https://zenodo.org/record/8189110/files/Supplemental%20Table%20S2.xlsx?download=1

Table S3 : **Transcription factor binding site enrichment analysis.** Columns represent: 1-Transcription factor binding site motif ID, 2- P-value of motif enrichment in 1000 nucleotide regions of the genes up-regulated in NT-3 condition as compared to NGF condition obtained by Fisher count test, 2- percentage of promoter regions of all genes expressed in the neurons containing at least one motif, 3- percentage of promoter regions of the genes up-regulated in NT-3 condition compared to NGF condition containing at least one motif, 5- ratios of fractions of genes up-regulated in NT-3 condition as compared to NGF condition exhibiting a motif compared to all expressed genes, 6-9- same as 2-5 for genes up-regulated in NGF condition compared to NT-3 condition, 10- ratios of genes up-regulated in NGF condition exhibiting a motif in promoter-region compared to genes up-regulated in NT-3 condition, 11- ratios of genes up-regulated in NT-3 condition exhibiting a motif in promoter-region compared to genes up-regulated in NGF condition.
https://zenodo.org/record/8189110/files/Supplemental%20Table%20S3.xlsx?download=1

Table S4 : **Distal-to-proximal promoter 3' UTR shifts in cell bodies of NGF treated cells compared to NT-3.** Columns represent: 1- Ensembl Rn5 transcript ID, 2- gene symbol, 3- ID of the promoter-proximal 3' UTR isoform (Ip), 4- ID of the promoter-distal 3' UTR isoform (Id), 5- difference in relative promoter-proximal (Ip/Ip+Id) usage in the cell body compartment between NGF and NT-3 condition, 6- relative promoter-proximal (Ip/Ip+Id) usage in the cell body compartment of NGF-treated condition, 7- relative promoter-proximal (Ip/Ip+Id) usage in the cell body compartment of NT-3-treated condition, 8- normalised read-count for promoter-proximal (Ip) 3' UTR isoform in the cell body of NGF condition, 9- normalised read-count for promoter-distall (Id) 3' UTR isoform in the cell body of NGF condition, 10- normalised read-count for promoter-proximal (Ip) 3' UTR isoform in the cell body of NT-3 condition, 11- normalised read-count for promoter-distall (Id) 3' UTR isoform in the cell body of NT-3 condition, 12- binary value indicating whether significant promoter-distal shift in NT-3 condition, 13-binary value indicating whether significant promoter-proximal shift in NGF.
https://zenodo.org/record/8189110/files/Supplemental%20Table%20S4.xlsx?download=1

Table S5 : **Distal-to-proximal promoter 3' UTR shifts in cell bodies of NT-3 treated cells compared to NGF.** Columns represent: 1- Ensembl Rn5 transcript ID, 2- gene symbol, 3- ID of the promoter-proximal 3' UTR isoform (Ip), 4- ID of the promoter-distal 3' UTR isoform (Id), 5- difference in relative promoter-proximal (Ip/Ip+Id) usage in the cell body compartment between NGF and NT-3 condition, 6- relative promoter-proximal (Ip/Ip+Id) usage in the cell body compartment of NGF-treated condition, 7- relative promoter-proximal (Ip/Ip+Id) usage in the cell

body compartment of NT-3-treated condition, 8- normalised read-count for promoter-proximal (Ip) 3' UTR isoform in the cell body of NGF condition, 9- normalised read-count for promoter-distall (Id) 3' UTR isoform in the cell body of NGF condition, 10- normalised read-count for promoter-proximal (Ip) 3' UTR isoform in the cell body of NT-3 condition, 11- normalised read-count for promoter-distall (Id) 3' UTR isoform in the cell body of NT-3 condition, 12- binary value indicating whether significant promoter-distal shift in NT-3 condition, 13-binary value indicating whether significant promoter-proximal shift in NGF.
https://zenodo.org/record/8189110/files/Supplemental%20Table%20S5.xlsx?download=1

Table S6 : **Description of the publicly available CLIP sequencing data generated in human cell lines against 126 RBPs.** Columns represent: 1- CLIP experiment ID, 2- Human protein symbol of the clipped RNA binding protein (RBP), 3- Rat Rn5 gene symbol of the clipped RBP, 4- Z-score of the propensity of the clipped RBP to localize into cellular condensates as predicted by GraPES (Kuechler et al. 2022), 5- Change in gene expression between NGF and NT-3 treated condition (log2FC), 6- P-value (FDR) of the significance in detected changes in gene expression between NGF and NT-3, 7- difference in axonal localisation score between NGF and NT-3 condition, 8- predicted axonal localisation score in NGF condition, 9- predicted axonal localisation score in NT-3 condition, 10- averaged gene expression in cell body of NGF condition, 11- averaged gene expression in cell body of NT-3 condition, 12- averaged gene expression in axons of NGF condition, 13- averaged gene expression in axons of NT-3 condition.
https://zenodo.org/record/8189110/files/Supplemental%20Table%20S6.xlsx?download=1

Table S7 : **17 predicted positive regulators of polyadenylation.** Columns represent: 1- CLIP experiment ID, 2- human protein symbol of the clipped RBP, 3- position (start) relative to the promoter-proximal (Ip) 3' end where RBP is most significantly associated with promoter-proximal 3' UTR isoform relative usage, 4- position (end) relative to the promoter-proximal (Ip) 3' end where RBP is most significantly associated with promoter-proximal 3' UTR isoform relative usage, 5- position (start) relative to the promoter-distal (Id) 3' end where RBP is most significantly associated with promoter-distal 3' UTR isoform relative usage, 6- position (end) relative to the promoter-distal (Id) 3' end where RBP is most significantly associated with promoter-distal 3' UTR isoform relative usage, 7- maximum P-value of association (Welch's t-test) between RBP cross-link event and promoter-proximal (Ip) 3' UTR isoform relative usage. 8- maximum P-value of association (Welch's t-test) between RBP cross-link event and promoter-distal (Id) 3' UTR isoform relative usage,9-10- snapshot of the protein-protein interaction network as obtained from STRING (Szklarczyk et al. 2011) , 11- human protein symbol of the clipped RNA binding protein (RBP),

12- Rat Rn5 gene symbol of the clipped RBP, 13- Z-score of the propensity of the clipped RBP to localize into cellular condensates as predicted by GraPES (Kuechler et al. 2022), 14- Change in gene expression between NGF and NT-3 treated condition (log2FC), 15- P-value (FDR) of the significance in detected changes in gene expression between NGF and NT-3, 16- difference in axonal localisation score between NGF and NT-3 condition, 17- predicted axonal localisation score in NGF condition, 18- predicted axonal localisation score in NT-3 condition, 19- averaged gene expression in cell body of NGF condition, 20- averaged gene expression in cell body of NT-3 condition, 21- averaged gene expression in axons of NGF condition, 22- averaged gene expression in axons of NT-3 condition.
https://zenodo.org/record/8189110/files/Supplemental%20Table%20S7.xlsx?download=1

Table S8 : **27 predicted negative regulators of the short 3' UTR and positive regulators of the long 3' UTR.** Columns represent: 1- CLIP experiment ID, 2- human protein symbol of the clipped RBP, 3- position (start) relative to the promoter-proximal (Ip) 3' end where RBP is most significantly associated with promoter-proximal 3' UTR isoform relative usage, 4- position (end) relative to the promoter-proximal (Ip) 3' end where RBP is most significantly associated with promoter-proximal 3' UTR isoform relative usage, 5- position (start) relative to the promoter-distal (Id) 3' end where RBP is most significantly associated with promoter-distal 3' UTR isoform relative usage, 6- position (end) relative to the promoter-distal (Id) 3' end where RBP is most significantly associated with promoter-distal 3' UTR isoform relative usage, 7- maximum P-value of association (Welch's t-test) between RBP cross-link event and promoter-proximal (Ip) 3' UTR isoform relative usage. 8- maximum P-value of association (Welch's t-test) between RBP cross-link event and promoter-distal (Id) 3' UTR isoform relative usage, 9-10- enriched biological pathway as obtained from STRING (Szklarczyk et al. 2011) along with snapshot of the protein-protein interaction network, 11- human protein symbol of the clipped RNA binding protein (RBP), 12- Rat Rn5 gene symbol of the clipped RBP, 13- Z-score of the propensity of the clipped RBP to localize into cellular condensates as predicted by GraPES (Kuechler et al. 2022), 14- Change in gene expression between NGF and NT-3 treated condition (log2FC), 15- P-value (FDR) of the significance in detected changes in gene expression between NGF and NT-3, 16- difference in axonal localisation score between NGF and NT-3 condition, 17- predicted axonal localisation score in NGF condition, 18- predicted axonal localisation score in NT-3 condition, 19- averaged gene expression in cell body of NGF condition, 20- averaged gene expression in cell body of NT-3 condition, 21- averaged gene expression in axons of NGF condition, 22- averaged gene expression in axons of NT-3 condition.
https://zenodo.org/record/8189110/files/Supplemental%20Table%20S8.xlsx?download=1

Table S9 : **Modelling of axonal localisation score.** Columns represent: 1- 3' UTR isoform unique ID, 2- Rn5 rat gene symbol, 3- Ensembl Rn5 transcript ID, 4- predicted difference in axonal localisation score between NGF and NT-3, 5- predicted axonal localisation score in NGF, 6- predicted axonal localisation score in NT-3, 7- ratio (log2) of normalised read count between axons and cell body in NGF, 8- ratio (log2) of normalised read count between axons and cell body in NT-3, 9- average read count in cell bodies of NGF, 10- average read count in cell bodies of NT-3, 11- average read count in axons of NGF, 12- average read count in axons of NT-3, 13- normalised read count in cell body sample 1 of NGF condition, 14- normalised read count in cell body sample 2 of NGF condition, 15- normalised read count in axonal sample 1 of NGF condition, 16- normalised read count in axonal sample 2 of NGF condition, 17- normalised read count in cell body sample 1 of NT-3 condition, 18- normalised read count in cell body sample 2 of NT-3 condition, 19- normalised read count in axonal sample 1 of NT-3 condition, 20- normalised read count in axonal sample 2 of NT-3 condition.
https://zenodo.org/record/8189110/files/Supplemental%20Table%20S9.xlsx?download=1

Table S10 : **Over-transported transcripts in NGF-treated axons as compared to NT-3 treated axons.** Columns represent: 1- Coordinate of the 3' UTR isoform in Rn5, 2- 3' UTR isoform unique ID, 3- Rn5 rat gene symbol, 4- Ensembl Rn5 transcript ID, 5- predicted difference in axonal localisation score between NGF and NT-3, 6- predicted difference in relative abundance ratios (ax/cb) between NGF and NT-3, 7- predicted axonal localisation score in NGF, 8- predicted axonal localisation score in NT-3, 9- average read count in cell bodies of NGF, 10- average read count in cell bodies of NT-3, 11- average read count in axons of NGF, 12- average read count in axons of NT-3, 13- transcript length (nucleotide).
https://zenodo.org/record/8189110/files/Supplemental%20Table%20S10.xlsx?download=1

Table S11 : **Over-transported transcripts in NT-3 treated axons as compared to NGF-treated axons.** Columns represent: 1- Coordinate of the 3' UTR isoform in Rn5, 2- 3' UTR isoform unique ID, 3- Rn5 rat gene symbol, 4- Ensembl Rn5 transcript ID, 5- predicted difference in axonal localisation score between NGF and NT-3, 6- predicted difference in relative abundance ratios (ax/cb) between NGF and NT-3, 7- predicted axonal localisation score in NGF, 8- predicted axonal localisation score in NT-3, 9- average read count in cell bodies of NGF, 10- average read count in cell bodies of NT-3, 11- average read count in axons of NGF, 12- average read count in axons of NT-3, 13- transcript length (nucleotide).
https://zenodo.org/record/8189110/files/Supplemental%20Table%20S11.xlsx?download=1

Table S12 : **Positive RBP regulators of axonal localisation.** Columns represent: 1- CLIP sequencing experiment ID, 2- Human protein symbol of the clipped RNA binding protein (RBP), 3- Rat Rn5 gene symbol of the clipped RBP, 4- Z-score of the propensity of the clipped RBP to localize into cellular condensates as predicted by GraPES (Kuechler et al. 2022), 5- Change in gene expression between NGF and NT-3 treated condition (log2FC), 6- P-value (FDR) of the significance in detected changes in gene expression between NGF and NT-3, 7- difference in axonal localisation score between NGF and NT-3 condition, 8- predicted axonal localisation score in NGF condition, 9- predicted axonal localisation score in NT-3 condition, 10- averaged gene expression in cell body of NGF condition, 11- averaged gene expression in cell body of NT-3 condition, 12- averaged gene expression in axons of NGF condition, 13- averaged gene expression in axons of NT-3 condition.
https://zenodo.org/record/8189110/files/Supplemental%20Table%20S12.xlsx?download=1

Table S13 : **Negative RBP regulators of axonal localisation.** Columns represent: 1- CLIP sequencing experiment ID, 2- Human protein symbol of the clipped RNA binding protein (RBP), 3- Rat Rn5 gene symbol of the clipped RBP, 4- Z-score of the propensity of the clipped RBP to localize into cellular condensates as predicted by GraPES (Kuechler et al. 2022), 5- Change in gene expression between NGF and NT-3 treated condition (log2FC), 6- P-value (FDR) of the significance in detected changes in gene expression between NGF and NT-3, 7- difference in axonal localisation score between NGF and NT-3 condition, 8- predicted axonal localisation score in NGF condition, 9- predicted axonal localisation score in NT-3 condition, 10- averaged gene expression in cell body of NGF condition, 11- averaged gene expression in cell body of NT-3 condition, 12- averaged gene expression in axons of NGF condition, 13- averaged gene expression in axons of NT-3 condition. Included in the Table are the enriched biological pathway as obtained from STRING (Szklarczyk et al. 2011) along with snapshot of the protein-protein interaction network.
https://zenodo.org/record/8189110/files/Supplemental%20Table%20S13.xlsx?download=1

Table S14 : **Promoter-proximal shifts in NGF-treated axons as compared to cell bodies.** Columns represent: 1- Ensembl Rn5 transcript ID, 2- Rat Rn5 gene symbol, 3- promoter-proximal (Ip) 3' UTR isoform ID, 4- promoter-distal (Id) 3' UTR isoform ID, 5- difference in relative promoter-proximal usage between axons and cell bodies in NGF, 6- relative promoter-proximal usage in NGF axons, 7- relative promoter-proximal usage in NGF cell bodies, 8- difference in promoter-proximal and promoter-distal ratios (log2) between cell bodies and axons in NGF, 9- promoter-proximal and promoter-distal ratios (log2) in axons NGF, 10- promoter-proximal and promoter-distal ratios (log2) in cell bodies NGF, 11- P-value of the difference in relative promoter-proximal usage between axons and cell bodies in NGF (Fisher

count test; FDR corrected), 12- Read count of the promoter-proximal 3' UTR isoform (Ip) in cell body NGF, 13- Read count of the promoter-distal 3' UTR isoform (Id) in cell body NGF, 14- Read count of the promoter-proximal 3' UTR isoform (Ip) in axons NGF, 15- Read count of the promoter-distal 3' UTR isoform (Id) in axons NGF.
https://zenodo.org/record/8189110/files/Supplemental%20Table%20S14.xlsx?download=1

**Table S15 : Promoter-proximal shifts in NT-3 treated axons as compared to cell bodies.** Columns represent: 1- Ensembl Rn5 transcript ID, 2- Rat Rn5 gene symbol, 3- promoter-proximal (Ip) 3' UTR isoform ID, 4- promoter-distal (Id) 3' UTR isoform ID, 5- difference in relative promoter-proximal usage between axons and cell bodies in NT-3, 6- relative promoter-proximal usage in NT-3 axons, 7- relative promoter-proximal usage in NNT-3GF cell bodies, 8- difference in promoter-proximal and promoter-distal ratios (log2) between cell bodies and axons in NT-3, 9- promoter-proximal and promoter-distal ratios (log2) in axons NT-3, 10- promoter-proximal and promoter-distal ratios (log2) in cell bodies NT-3, 11- P-value of the difference in relative promoter-proximal usage between axons and cell bodies in NT-3 (Fisher count test; FDR corrected), 12- Read count of the promoter-proximal 3' UTR isoform (Ip) in cell body NT-3, 13- Read count of the promoter-distal 3' UTR isoform (Id) in cell body NT-3, 14- Read count of the promoter-proximal 3' UTR isoform (Ip) in axons NT-3, 15- Read count of the promoter-distal 3' UTR isoform (Id) in axons NT-3.
https://zenodo.org/record/8189110/files/Supplemental%20Table%20S15.xlsx?download=1

Table S16 : **Promoter-distal shifts in NGF-treated axons as compared to cell bodies.** Columns represent: 1- Ensembl Rn5 transcript ID, 2- Rat Rn5 gene symbol, 3- promoter-proximal (Ip) 3' UTR isoform ID, 4- promoter-distal (Id) 3' UTR isoform ID, 5- difference in relative promoter-proximal usage between axons and cell bodies in NGF, 6- relative promoter-proximal usage in NGF axons, 7- relative promoter-proximal usage in NGF cell bodies, 8- difference in promoter-proximal and promoter-distal ratios (log2) between cell bodies and axons in NGF, 9- promoter-proximal and promoter-distal ratios (log2) in axons NGF, 10- promoter-proximal and promoter-distal ratios (log2) in cell bodies NGF, 11- P-value of the difference in relative promoter-proximal usage between axons and cell bodies in NGF (Fisher count test; FDR corrected), 12- Read count of the promoter-proximal 3' UTR isoform (Ip) in cell body NGF, 13- Read count of the promoter-distal 3' UTR isoform (Id) in cell body NGF, 14- Read count of the promoter-proximal 3' UTR isoform (Ip) in axons NGF. 15- Read count of the promoter-distal 3' UTR isoform (Id) in axons NGF.
https://zenodo.org/record/8189110/files/Supplemental%20Table%20S16.xlsx?download=1

**Table S17 : Promoter-distal shifts in NT-3 treated axons as compared to cell bodies.** Columns represent: 1- Ensembl Rn5 transcript ID, 2- Rat Rn5 gene symbol, 3- promoter-proximal (Ip) 3' UTR isoform ID, 4- promoter-distall (Id) 3' UTR isoform ID, 5- difference in relative promoter-proximal usage between axons and cell bodies in NT-3, 6- relative promoter-proximal usage in NT-3 axons, 7- relative promoter-proximal usage in NNT-3GF cell bodies, 8- difference in promoter-proximal and promoter-distal ratios (log2) between cell bodies and axons in NT-3, 9- promoter-proximal and promoter-distal ratios (log2) in axons NT-3, 10- promoter-proximal and promoter-distal ratios (log2) in cell bodies NT-3, 11- P-value of the difference in relative promoter-proximal usage between axons and cell bodies in NT-3 (Fisher count test; FDR corrected), 12- Read count of the promoter-proximal 3' UTR isoform (Ip) in cell body NT-3, 13- Read count of the promoter-distal 3' UTR isoform (Id) in cell body NT-3, 14- Read count of the promoter-proximal 3' UTR isoform (Ip) in axons NT-3, 15- Read count of the promoter-distal 3' UTR isoform (Id) in axons NT-3.
https://zenodo.org/record/8189110/files/Supplemental%20Table%20S17.xlsx?download=1

Table S18 : **Candidate axonal remodeling in NGF.** Columns represent: 1- Ensembl Rn5 transcript ID, 2- Rat Rn5 gene symbol, 3- promoter-proximal (Ip) 3' UTR isoform ID, 4- promoter-distall (Id) 3' UTR isoform ID, 5- difference in relative promoter-proximal usage between axons and cell bodies in NGF, 6- relative promoter-proximal usage in NGF axons, 7- relative promoter-proximal usage in NGF cell bodies, 8- difference in promoter-proximal and promoter-distal ratios (log2) between cell bodies and axons in NGF, 9- promoter-proximal and promoter-distal ratios (log2) in axons NGF, 10- promoter-proximal and promoter-distal ratios (log2) in cell bodies NGF, 11- P-value of the difference in relative promoter-proximal usage between axons and cell bodies in NGF (Fisher count test; FDR corrected), 12- Read count of the promoter-proximal 3' UTR isoform (Ip) in cell body NGF, 13- Read count of the promoter-distal 3' UTR isoform (Id) in cell body NGF, 14- Read count of the promoter-proximal 3' UTR isoform (Ip) in axons NGF. 15- Read count of the promoter-distal 3' UTR isoform (Id) in axons NGF.
https://zenodo.org/record/8189110/files/Supplemental%20Table%20S18.xlsx?download=1

Table S19 : **Candidate axonal remodeling in NT-3.** Columns represent: 1- Ensembl Rn5 transcript ID, 2- Rat Rn5 gene symbol, 3- promoter-proximal (Ip) 3' UTR isoform ID, 4- promoter-distall (Id) 3' UTR isoform ID, 5- difference in relative promoter-proximal usage between axons and cell bodies in NT-3, 6- relative promoter-proximal usage in NT-3 axons, 7- relative promoter-proximal usage in NNT-3GF cell bodies, 8- difference in promoter-proximal and promoter-distal ratios (log2) between cell bodies and axons in NT-3, 9- promoter-proximal and promoter-distal ratios (log2) in axons NT-3, 10- promoter-proximal and promoter-distal

ratios (log2) in cell bodies NT-3, 11- P-value of the difference in relative promoter-proximal usage between axons and cell bodies in NT-3 (Fisher count test; FDR corrected), 12- Read count of the promoter-proximal 3' UTR isoform (Ip) in cell body NT-3, 13- Read count of the promoter-distal 3' UTR isoform (Id) in cell body NT-3, 14- Read count of the promoter-proximal 3' UTR isoform (Ip) in axons NT-3, 15- Read count of the promoter-distal 3' UTR isoform (Id) in axons NT-3.
https://zenodo.org/record/8189110/files/Supplemental%20Table%20S19.xlsx?download=1

Table S20 : **NGF RBP regulators of axonal remodeling.** Columns content: 1- CLIP experiment ID, 2- position (start) relative to the promoter-proximal (Ip) 3' end where RBP is most significantly enriched in predicted remodelled 3' UTR isoforms in NGF condition, 3- position (end) relative to the promoter-proximal (Ip) 3' end where RBP is most significantly enriched in predicted remodelled 3' UTR isoforms in NGF condition, 4- maximum P-value of Fisher count enrichment test in RBP cross-link event in predicted remodelled promoter-proximal (Ip) 3' UTR isoforms in NGF condition, 5-6- enriched biological pathway as obtained from STRING (Szklarczyk et al. 2011) along with snapshot of the protein-protein interaction network, 7- human protein symbol of the clipped RNA binding protein (RBP), 8- Rat Rn5 gene symbol of the clipped RBP, 9- Z-score of the propensity of the clipped RBP to localize into cellular condensates as predicted by GraPES (Kuechler et al. 2022), 10- Change in gene expression between NGF and NT-3 treated condition (log2FC), 11- P-value (FDR) of the significance in detected changes in gene expression between NGF and NT-3, 12- difference in axonal localisation score between NGF and NT-3 condition, 13- predicted axonal localisation score in NGF condition, 14- predicted axonal localisation score in NT-3 condition, 15- averaged gene expression in cell body of NGF condition, 16- averaged gene expression in cell body of NT-3 condition, 17- averaged gene expression in axons of NGF condition, 18- averaged gene expression in axons of NT-3 condition.
https://zenodo.org/record/8189110/files/Supplemental%20Table%20S20.xlsx?download=1

Table S21 : **NT-3 RBP regulators of axonal remodeling.** Columns content: 1- CLIP experiment ID, 2- position (start) relative to the promoter-proximal (Ip) 3' end where RBP is most significantly enriched in predicted remodelled 3' UTR isoforms in NT-3 condition, 3- position (end) relative to the promoter-proximal (Ip) 3' end where RBP is most significantly enriched in predicted remodelled 3' UTR isoforms in NT-3 condition, 4- maximum P-value of Fisher count enrichment test in RBP cross-link event in predicted remodelled promoter-proximal (Ip) 3' UTR isoforms in NT-3 condition, 5-6- enriched biological pathway as obtained from STRING (Szklarczyk et al. 2011) along with snapshot of the protein-protein interaction network, 7-

human protein symbol of the clipped RNA binding protein (RBP), 8- Rat Rn5 gene symbol of the clipped RBP, 9- Z-score of the propensity of the clipped RBP to localize into cellular condensates as predicted by GraPES (Kuechler et al. 2022), 10- Change in gene expression between NGF and NT-3 treated condition (log2FC), 11- P-value (FDR) of the significance in detected changes in gene expression between NGF and NT-3, 12- difference in axonal localisation score between NGF and NT-3 condition, 13- predicted axonal localisation score in NGF condition, 14- predicted axonal localisation score in NT-3 condition, 15- averaged gene expression in cell body of NGF condition, 16- averaged gene expression in cell body of NT-3 condition, 17- averaged gene expression in axons of NGF condition, 18- averaged gene expression in axons of NT-3 condition.
https://zenodo.org/record/8189110/files/Supplemental%20Table%20S21.xlsx?download=1

Table S22 : **ANOVA linear model of axonal localisation.** Columns content: 1- name of the linear model, 2- full description of the model, 3- degree of freedom, 4- AIC as obtained from ANOVA comparing all models, 5- analysis of variance table comparing models in NGF condition, 6- analysis of variance table comparing models in NT-3 condition.
https://zenodo.org/record/8189110/files/Supplemental%20Table%20S22.xlsx?download=1

Table S23: **Primers and PCR conditions.** Columns content: 1- names of the primers, 2- full sequence, 3- NCBI accession number, 4-Total magnesium concentration in the PCR mix, 5-Temperature for annealing step in PCR program, 6-application for which primer set was used

| Primers names | Sequences | NCBI Accession number | [Mg++] | Tann. | Application |
|---|---|---|---|---|---|
| HistoneH4 108–Fwd | ACGCCTGTGGTCTTCAATCAGG | M27433 | 2.5mM | 56°C | RT-PCR |
| HistoneH4 337–Rev | GCGGGTCTCCTCGTAGATGAG | | | | |
| | | | | | |
| R bact 82-F | ATGGATGACGATATCGCTGCG | NM_031144.3 | 2.5mM | 56ºC | RT-PCR |
| R bact 292-R | GGTGACAATGCCGTGTTCAAT | | | | |
| | | | | | |

| | | | | | |
|---|---|---|---|---|---|
| Rab22a_F1 | TGAAGGGTCAGAACTCCACGGAGTC | XM_001064863.7 | n/a | 60°C | RT-qPCR |
| Rab22a_R1 | CACATAGATGCTGTTGTGAAAGGCACC | | | | |
| | | | | | |
| Eid2_F1 | GAGGCAGTGCATCGCTGGAGG | ENSRNOT00000079113.1 | n/a | 60°C | RT-qPCR |
| Eid2_R1 | TTTACTTATTAACGAAGCCACGAGGATGG | | | | |
| | | | | | |
| B2M 239F | CTGTCCTTCAGCAAGGACTGG | ENSRNOT00000023017 | n/a | 60°C | RT-qPCR |
| B2M 394-R | TCCATAGAGCTTGATTACATGTCTCGG | | | | |

**References**


Andreassi C, Luisier R, Crerar H, Darsinou M, Blokzijl-Franke S, Lenn T, Luscombe NM, Cuda G, Gaspari M, Saiardi A, et al. 2021. Cytoplasmic cleavage of IMPA1 3' UTR is necessary for maintaining axon integrity. *Cell Rep* **34**: 108778.

Arnold P, Erb I, Pachkov M, Molina N, van Nimwegen E. 2012. MotEvo: integrated Bayesian probabilistic methods for inferring regulatory sites and motifs on multiple alignments of DNA sequences. *Bioinformatics* **28**: 487–494.

Baugh LR, Hill AA, Brown EL, Hunter CP. 2001. Quantitative analysis of mRNA amplification by in vitro transcription. *Nucleic Acids Res* **29**: E29.

Cleynen A, Koskas M, Lebarbier E, Rigaill G, Robin S. 2014. Segmentor3IsBack: an R package for the fast and exact segmentation of Seq-data. *Algorithms Mol Biol* **9**: 6.

Flicek P, Ahmed I, Amode MR, Barrell D, Beal K, Brent S, Carvalho-Silva D, Clapham P, Coates G, Fairley S, et al. 2013. Ensembl 2013. *Nucleic Acids Res* **41**: D48–55.

Hinrichs AS, Karolchik D, Baertsch R, Barber GP, Bejerano G, Clawson H, Diekhans M, Furey TS, Harte RA, Hsu F, et al. 2006. The UCSC Genome Browser Database: update 2006. *Nucleic Acids Res* **34**: D590–8.

Kuechler ER, Jacobson M, Mayor T, Gsponer J. 2022. GraPES: The Granule Protein Enrichment Server for prediction of biological condensate constituents. *Nucleic Acids Res*. http://dx.doi.org/10.1093/nar/gkac279.

Miura P, Shenker S, Andreu-Agullo C, Westholm JO, Lai EC. 2013. Widespread and

extensive lengthening of 3’ UTRs in the mammalian brain. *Genome Res* **23**: 812–825.

Robinson MD, McCarthy DJ, Smyth GK. 2010. edgeR: a Bioconductor package for differential expression analysis of digital gene expression data. *Bioinformatics* **26**: 139–140.

Szklarczyk D, Franceschini A, Kuhn M, Simonovic M, Roth A, Minguez P, Doerks T, Stark M, Muller J, Bork P, et al. 2011. The STRING database in 2011: functional interaction networks of proteins, globally integrated and scored. *Nucleic Acids Res* **39**: D561–8.